

Supporting Information

A Near-Infrared Small Molecule Coupled with Rigidity and Flexibility for High-Performance Multimodal Imaging-Guided Photodynamic and Photothermal Synergistic Therapy

Xiaozhen Li,^{‡ab} Fang Fang,^{‡c} Bo Sun,^d Chao Yin,^d Jihua Tan,^{ab} Yingpeng Wan,^{ab} Jinfeng Zhang,^{*c} Pengfei Sun,^d Quli Fan,^d Pengfei Wang,^{be} Shengliang Li^{*ab} and Chun-Sing Lee^{*ab}

^a Center of Super-Diamond and Advanced Films (COSDAF), Department of Chemistry, City University of Hong Kong, 83 Tat Chee Avenue, Kowloon, Hong Kong 999077, P. R. China

^b Joint Laboratory of Nano-organic Functional Materials and Devices (TIPC and CityU), City University of Hong Kong, 83 Tat Chee Avenue, Kowloon, Hong Kong SAR, P. R. China

^c Key Laboratory of Molecular Medicine and Biotherapy, School of Life Sciences, Beijing Institute of Technology, Beijing 100081, P. R. China

^d Key Laboratory for Organic Electronics and Information Displays& Jiangsu Key Laboratory for Biosensors, Institute of Advanced Materials (IAM), Jiangsu National Synergetic Innovation Center for Advanced Materials (SICAM), Nanjing University of Posts & Telecommunications, Nanjing 210023, P. R. China

^e Technical Institute of Physics and Chemistry, Chinese Academy of sciences, Beijing 100190, P.R. China

[‡] These authors contributed equally to this work.

*Corresponding authors

E-mail address: jfzhang@bit.edu.cn (J. F. Zhang)

lishengliang@iccas.ac.cn (S. L. Li)

apcslee@cityu.edu.hk (C.-S. LEE)

1. Supporting Figure

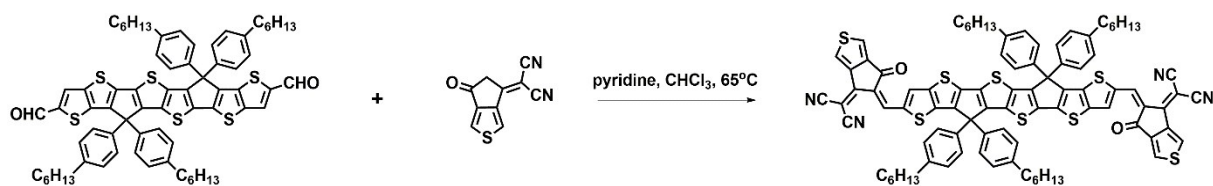


Fig. S1. The synthetic route of ETTC.

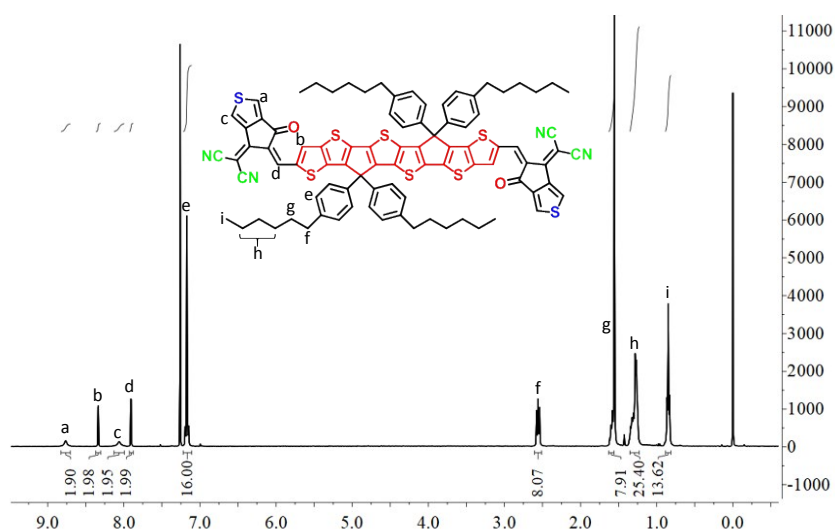


Fig. S2. ^1H NMR spectrum of ETTC in CDCl_3 .

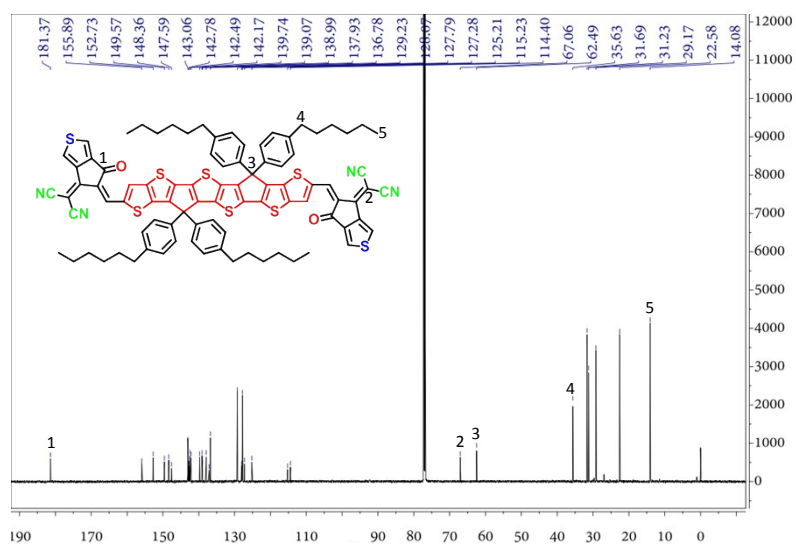


Fig. S3. ^{13}C NMR spectrum of ETTC in CDCl_3 .

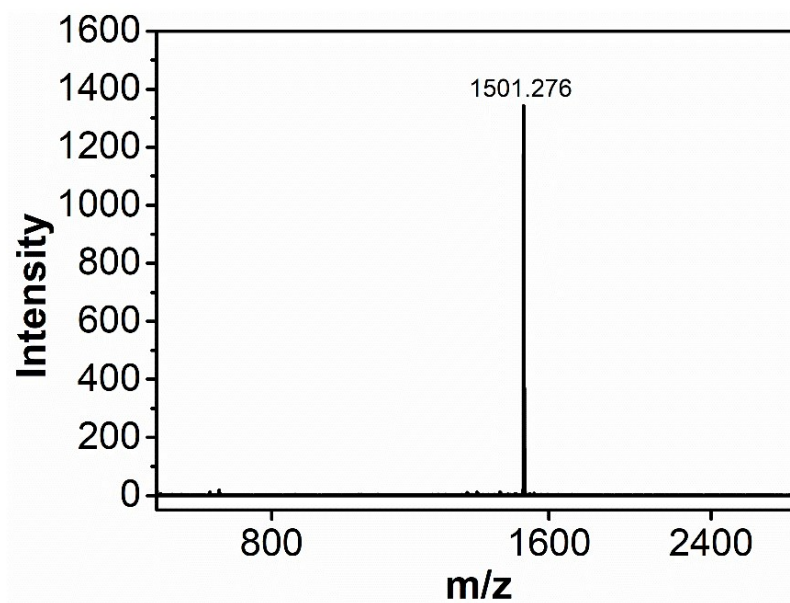


Fig. S4. A matrix assisted laser desorption/ionization time-of-flight (MALDI-TOF) mass spectrum of ETTC.

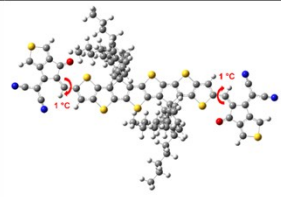
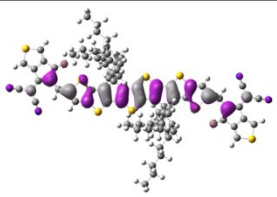
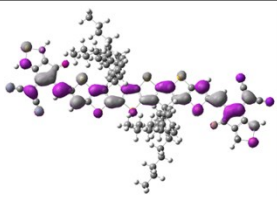
Optimized S_0 geometry	HOMO	LUMO	E_g	ΔE_{ST}
 ETTC	 -5.26 eV	 -3.43 eV	1.83 eV	0.65 eV

Fig. S5. Molecular information of ETTC calculated with DFT.

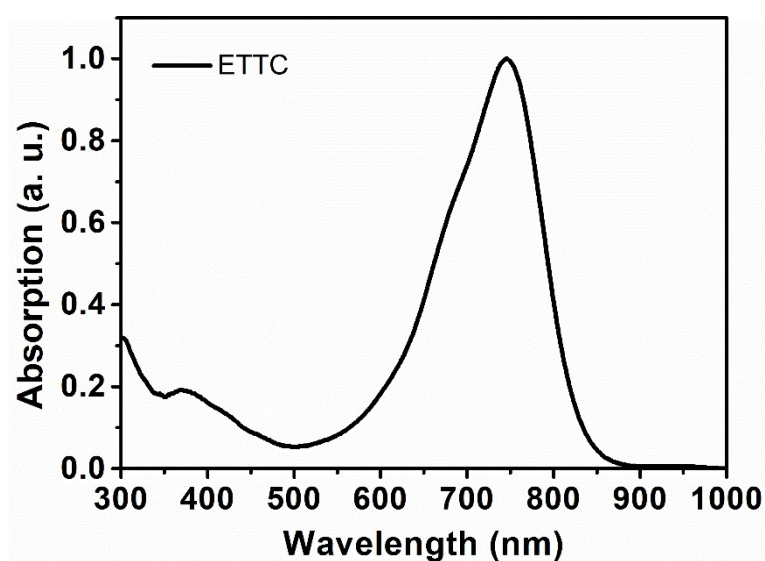


Fig. S6. Normalized absorption spectrum of ETTC in THF.

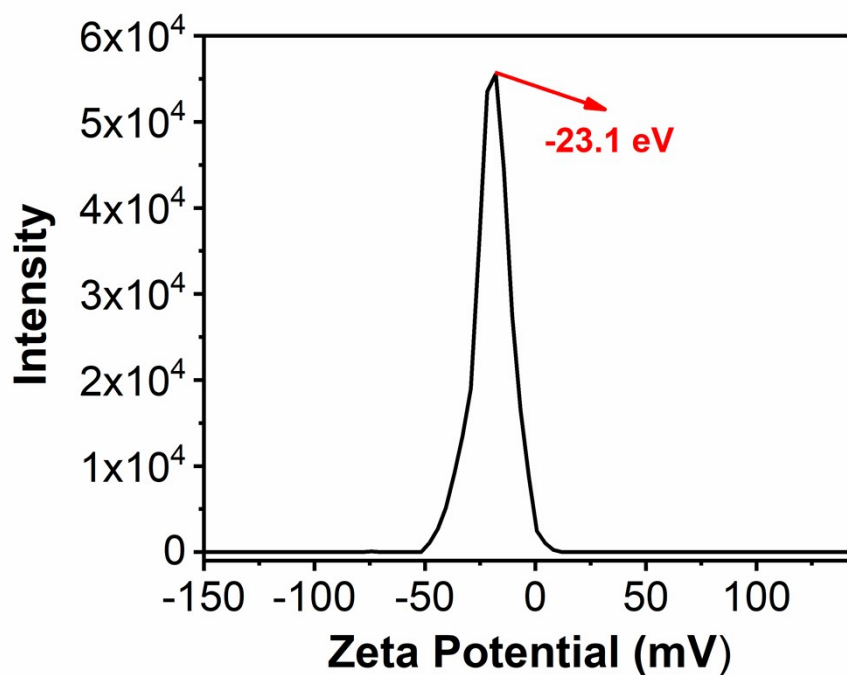


Fig. S7. Zeta potential of ETTTC NPs dispersed in DI water.

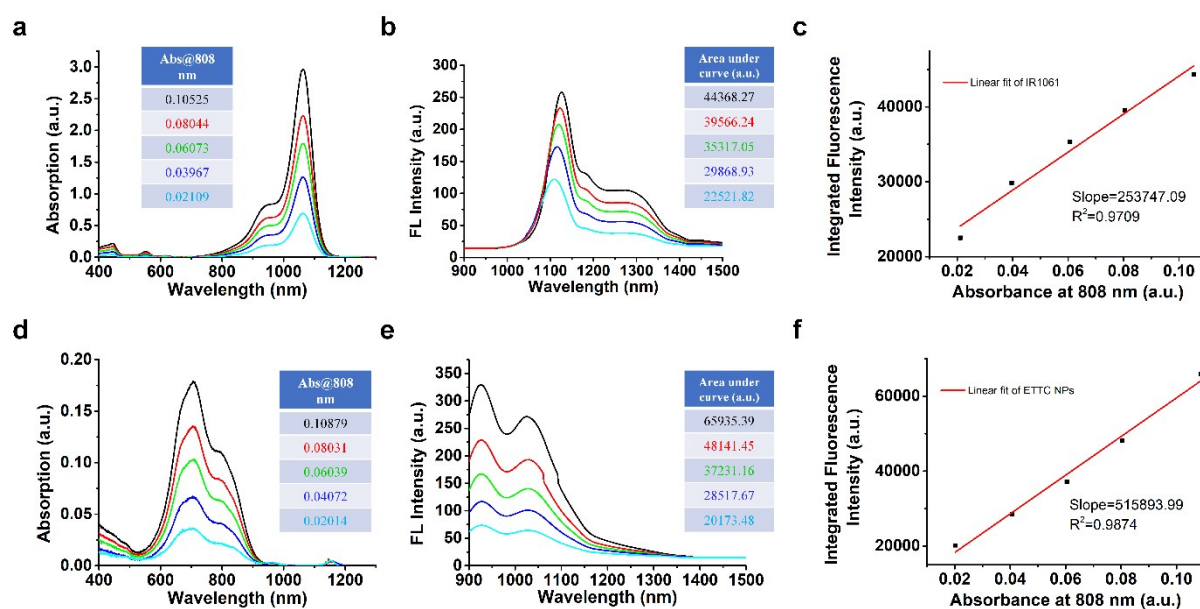


Fig. S8. a) Absorption spectra of IR1061 with OD values around 0.1, 0.08, 0.06, 0.04, and 0.02.

b) NIR- II emission spectra corresponding to IR1061 with OD values around 0.1, 0.08, 0.06,

0.04, and 0.02. c) Linear relationship between integrated fluorescence intensity (900-1500 nm) and absorbance value at 808 nm of IR1061. d) Absorption spectra of ETTC NPs with OD values around 0.1, 0.08, 0.06, 0.04, and 0.02. e) NIR- II emission spectra corresponding to ETTC NPs with OD values around 0.1, 0.08, 0.06, 0.04, and 0.02. f) Linear relationship between integrated fluorescence intensity (900-1500 nm) and absorbance value at 808 nm of ETTC NPs.

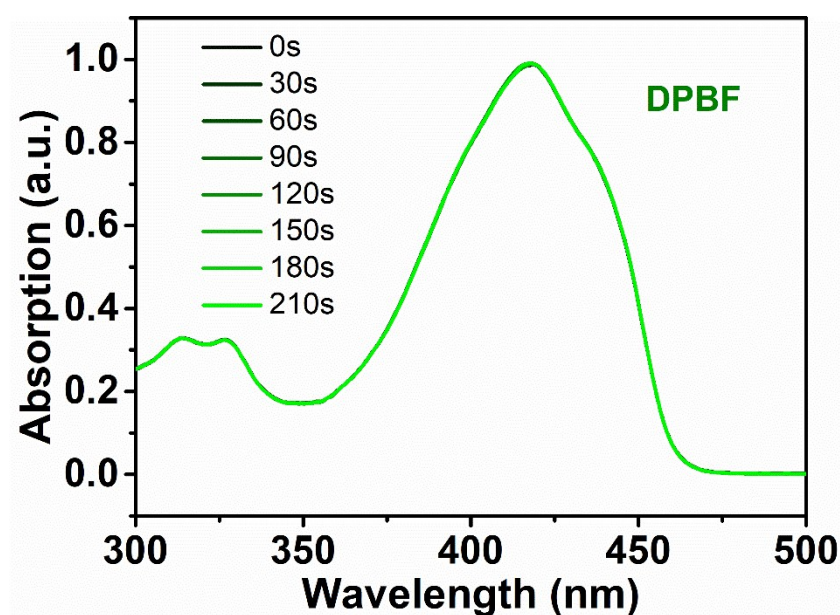


Fig. S9. Absorption change of DPBF itself with increasing irradiation time.

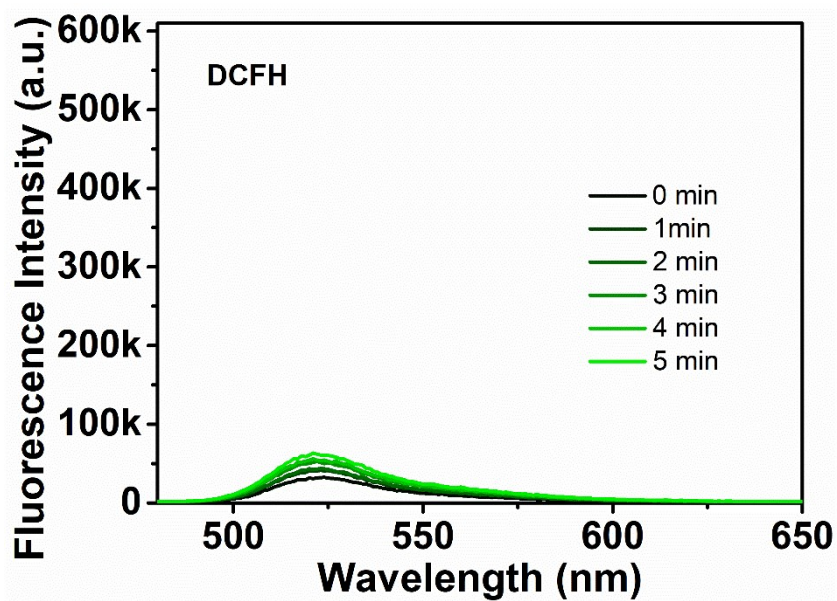


Fig. S10. Fluorescence intensity change of DCFH itself with increasing irradiation time.

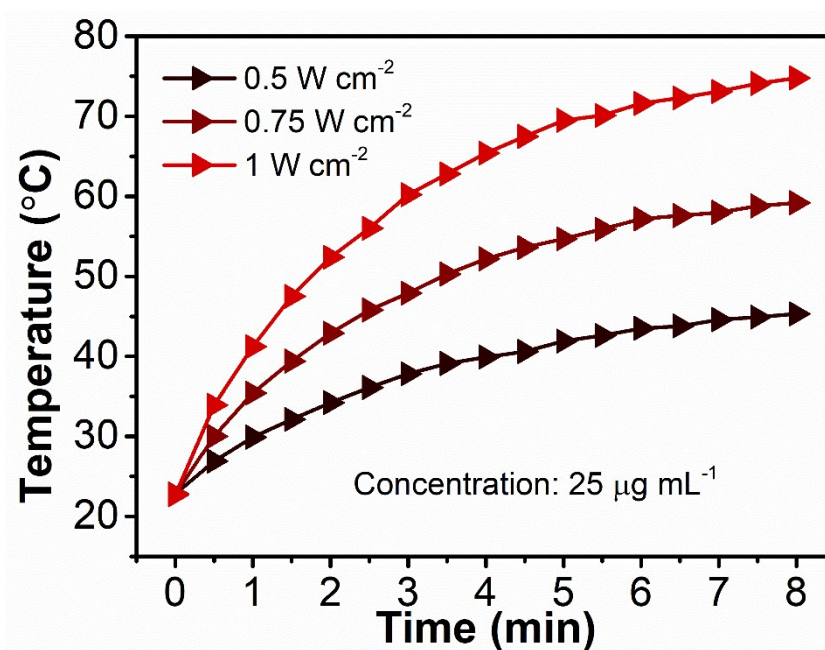


Fig. S11. Photothermal heating curves of ETTC NPs ($25 \mu\text{g mL}^{-1}$) under different laser powers as a function of time.

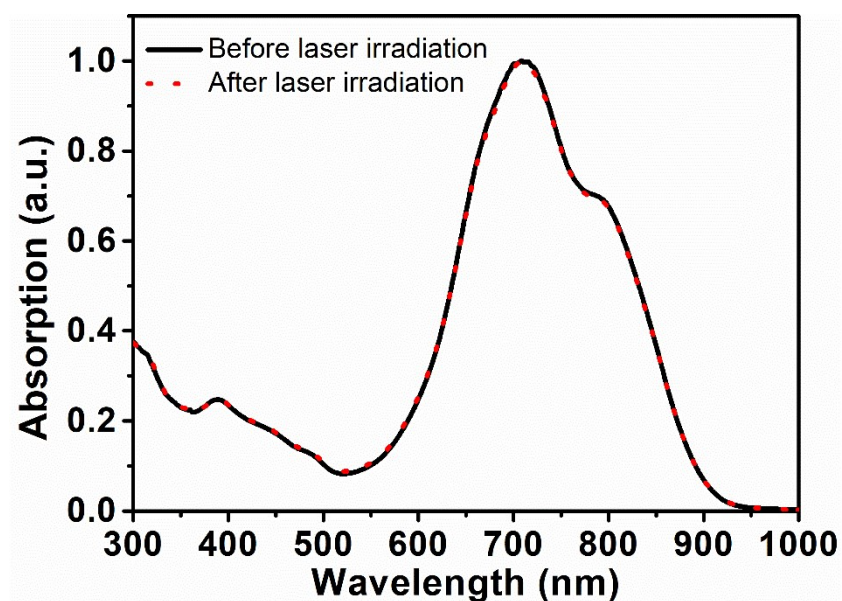


Fig. S12. Absorption change of ETTC NPs before and after laser irradiation (808 nm, 1 W cm^{-2} for 1 hour).

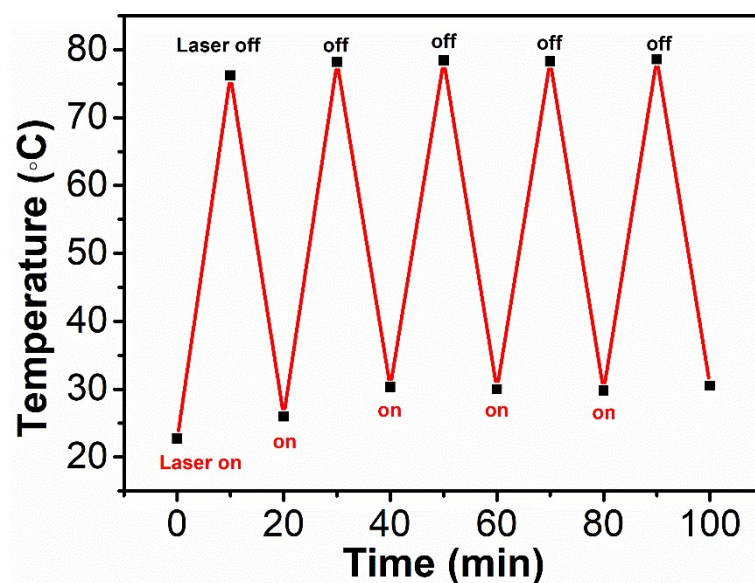


Fig. S13. Temperature variations of ETTC NPs under laser irradiation (1 W cm^{-2}) for 5 laser-on/off cycles.

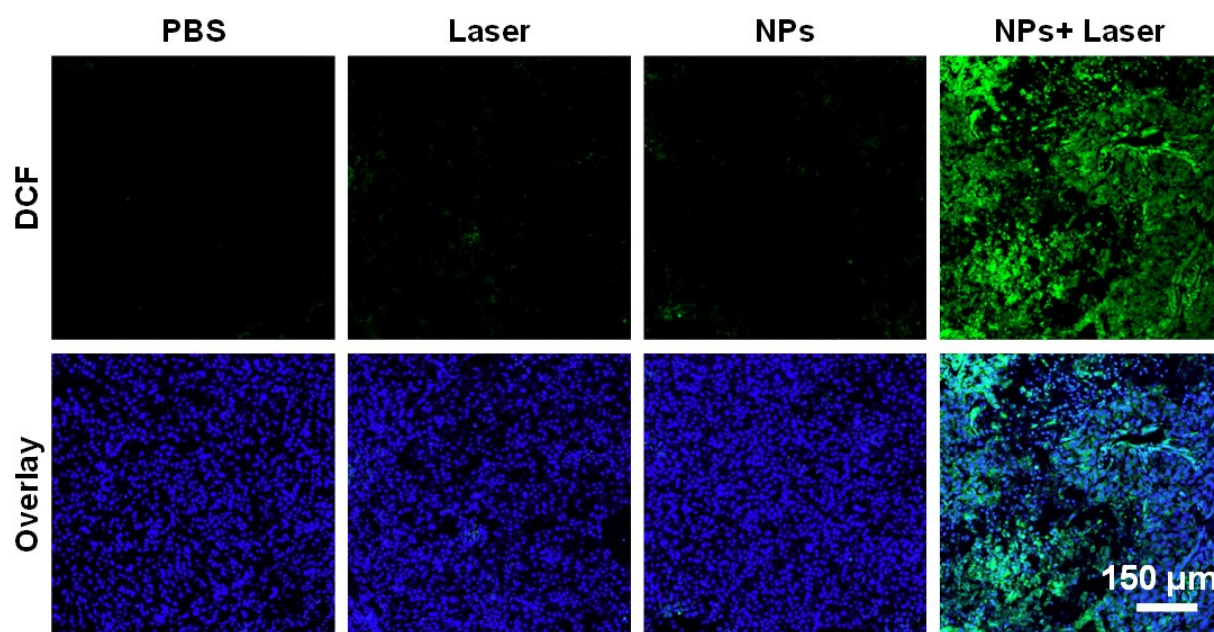


Fig. S14. *In vivo* ROS evaluation using ROS probe, DCFH-DA.

Table S1 Comparison of NIR-II imaging agents in aqueous solution under excitation at or beyond 808 nm.

Agent	Excitation wavelength	NIR-II fluorescent quantum yield (%)	PTT (photothermal conversion efficiency)	Photodynamic therapy	Photoacoustic imaging	Ref.
ETTC NPs	808 nm	3.0	52.8%	✓	✓	This work
IR-FTAP	808 nm	5.3	N/A	N/A	N/A	1
T-IPIC NPs	808 nm	2.2	39.6%	✓	N/A	2
IR-FEP	808 nm	2	N/A	N/A	N/A	3
IR-PEG NPs	808 nm	1.8	N/A	N/A	N/A	4
pDA-PEG	808 nm	1.7	N/A	N/A	N/A	5
P1-Pdots	808 nm	0.92	N/A	N/A	N/A	6
IR-E1	808 nm	0.7	N/A	N/A	N/A	7
CH1055-PEG	808 nm	0.3	N/A	N/A	N/A	8
CH-4T	808 nm	0.098	N/A	N/A	N/A	9
PBT NPs	980 nm	0.1	N/A	N/A	✓	10
FD-1080	1064 nm	0.31	N/A	N/A	N/A	11

2. Supporting Experimental Section

Photothermal conversion efficiency calculation

The photothermal conversion efficiency of ETTC NPs was determined referring to previously reported publications.^{12, 13} Briefly, ETTC NPs (25 µg mL⁻¹) were heated by 808 nm laser (1 W cm⁻²) for 10 min when its temperature reached a plateau. At this time point, the laser was shut off. The temperature in the cooling stage was monitored for 15 min when the temperature of ETTC NPs was close to the surrounding temperature. Identical measurements were also performed on DI water. The photothermal conversion efficiency was determined from Equation (a), and the other parameters in equation (a) were calculated from equation (b), (c) and (d).

$$\eta = \frac{hA(T_{Max}-T_{Surr})-Q_{Dis}}{I(1-10^{-A_{808}})} \quad (a)$$

$$\tau_S = \frac{m_D c_D}{hA} \quad (b)$$

$$t = -\tau_S \ln(\theta) = -\tau_S \ln\left(\frac{T_t - T_{Surr}}{T_{Max} - T_{Surr}}\right) \quad (c)$$

$$Q_{Dis} = \frac{c_D m_D (T_{Max(water)} - T_{Surr})}{\tau_{S(water)}} \quad (d)$$

In equation (a), η represents the heat transfer coefficient, A is the surface area of the container, T_{Max} and T_{Surr} are the plateau and surrounding temperature, respectively. Q_{Dis} is the heat dissipation from the light absorbed by the solvent and the sample cell, I denotes the incident laser power, and A_{808} is the absorbance of the sample at 808 nm. In equation (b), τ_S is the time constant for heat transfer of the system, m_D and c_D refer to the mass (0.5 g) and heat capacity (4.2 J g⁻¹) of DI water, separately, which was used to disperse the ETTC NPs. In equation (c), t is the time points in the cooling stage, T_t is the corresponding temperature of ETTC NPs during the cooling stage. In equation (d), τ_{water} is the time constant for heat transfer of the system.

NIR- II fluorescence quantum yield of ETTC NPs

The NIR- II fluorescence quantum yield (QY) of ETTC NPs was measured referring to the reported literature,¹⁴ in which the QY of IR1061 was reported to be $1.7 \pm 0.5\%$. Specifically, IR1061 in dichloromethane (DCM) was diluted with DCM to a series of concentrations until OD value at 808 nm reached to about 0.1, 0.08, 0.06, 0.04, and 0.02 (Fig. S4a). Then five corresponding NIR- II emission spectra were recorded in the region of 900-1500 nm under 808 nm laser irradiation (Fig. S4b). The fluorescence intensity was integrated in the 900-1500 nm region. Then the integrated fluorescence intensity was plotted against the OD value at 808 nm, from which the slope of IR1061 reference can be obtained (Fig. S4c). Similar measurements were carried on ETTC NPs in aqueous solution (Fig. S4d and Fig. S4e). Also, a slope for ETTC NPs can be determined (Fig. S4f). The QY of ETTC NPs is calculated to be $3.0 \pm 0.5\%$ according to the following equation, in which n_{sample} and n_{ref} represent the refractive index of DCM and water.

$$QY_{\text{sample}} = QY_{\text{ref}} \cdot \frac{\text{slope}_{\text{sample}}}{\text{slope}_{\text{ref}}} \cdot \left(\frac{n_{\text{sample}}}{n_{\text{ref}}} \right)^2$$

References

- 1 Q. Yang, Z. Hu, S. Zhu, R. Ma, H. Ma, Z. Ma, H. Wan, T. Zhu, Z. Jiang, W. Liu, L. Jiao, H. Sun, Y. Liang and H. Dai, *J. Am. Chem. Soc.*, 2018, **140**, 1715-1724.
- 2 Q. Wang, J. Xu, R. Geng, J. Cai, J. Li, C. Xie, W. Tang, Q. Shen, W. Huang and Q. Fan, *Biomaterials*, 2020, **231**, 119671.
- 3 Q. Yang, Z. Ma, H. Wang, B. Zhou, S. Zhu, Y. Zhong, J. Wang, H. Wan, A. Antaris, R. Ma, X. Zhang, J. Yang, X. Zhang, H. Sun, W. Liu, Y. Liang and H. Dai, *Adv. Mater.*, 2017, **29**, 1605497.
- 4 Z. Tao, G. Hong, C. Shinji, C. Chen, S. Diao, A. L. Antaris, B. Zhang, Y. Zou and H. Dai, *Angew. Chem. Int. Ed.*, 2013, **52**, 13002-13006.

- 5 G. Hong, Y. Zou, A. L. Antaris, S. Diao, D. Wu, K. Cheng, X. Zhang, C. Chen, B. Liu, Y. He, J. Z. Wu, J. Yuan, B. Zhang, Z. Tao, C. Fukunaga and H. Dai, *Nat. Commun.*, 2014, **5**, 4206.
- 6 Y. Liu, J. Liu, D. Chen, X. Wang, Z. Liu, H. Liu, L. Jiang, C. Wu and Y. Zou, *Macromolecules*, 2019, **52**, 5735-5740.
- 7 X.-D. Zhang, H. Wang, A. L. Antaris, L. Li, S. Diao, R. Ma, A. Nguyen, G. Hong, Z. Ma, J. Wang, S. Zhu, J. M. Castellano, T. Wyss-Coray, Y. Liang, J. Luo and H. Dai, *Adv. Mater.*, 2016, **28**, 6872-6879.
- 8 A. L. Antaris, H. Chen, K. Cheng, Y. Sun, G. Hong, C. Qu, S. Diao, Z. Deng, X. Hu, B. Zhang, X. Zhang, O. K. Yaghi, Z. R. Alamparambil, X. Hong, Z. Cheng and H. Dai, *Nat. Mater.*, 2016, **15**, 235-242.
- 9 A. L. Antaris, H. Chen, S. Diao, Z. Ma, Z. Zhang, S. Zhu, J. Wang, A. X. Lozano, Q. Fan, L. Chew, M. Zhu, K. Cheng, X. Hong, H. Dai and Z. Cheng, *Nat. Commun.*, 2017, **8**, 15269.
- 10 B. Guo, Z. Feng, D. Hu, S. Xu, E. Middha, Y. Pan, C. Liu, H. Zheng, J. Qian, Z. Sheng and B. Liu, *Adv. Mater.*, 2019, **31**, 1902504.
- 11 B. Li, L. Lu, M. Zhao, Z. Lei and F. Zhang, *Angew. Chem. Int. Ed.*, 2018, **57**, 7483-7487.
- 12 S. Li, X. Wang, R. Hu, H. Chen, M. Li, J. Wang, Y. Wang, L. Liu, F. Lv, X.-J. Liang and S. Wang, *Chem. Mater.*, 2016, **28**, 8669-8675.
- 13 X. Li, L. Liu, S. Li, Y. Wan, J.-X. Chen, S. Tian, Z. Huang, Y.-F. Xiao, X. Cui, C. Xiang, Q. Tan, X.-H. Zhang, W. Guo, X.-J. Liang and C.-S. Lee, *ACS Nano*, 2019, **13**, 12901-12911.
- 14 M. Casalboni, F. De Matteis, P. Prosposito, A. Quatela and F. Sarcinelli, *Chem. Phys. Lett.*, 2003, **373**, 372-378.